Developmental Cell, Volume *24*
Supplemental Information

Triacylglycerol Synthesis Enzymes Mediate Lipid Droplet Growth by Relocalizing from the ER to Lipid Droplets

Florian Wilfling, Huajin Wang, Joel T. Haas, Natalie Krahmer, Travis J. Gould, Aki Uchida, Ji-Xin Cheng, Morven Graham, Romain Christiano, Florian Fröhlich, Xinran Liu, Kimberly K. Buhman, Rosalind A. Coleman, Joerg Bewersdorf, Robert V. Farese, Jr., and Tobias C. Walther

Inventory of Supplemental Information

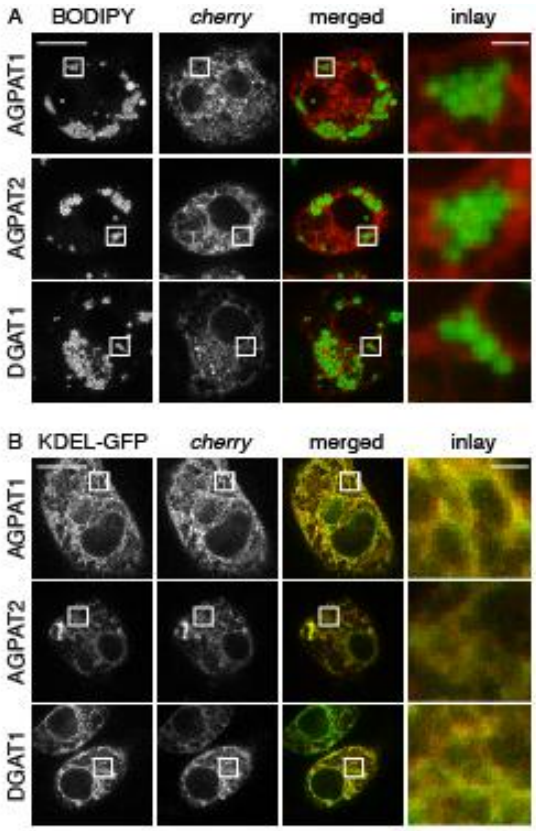

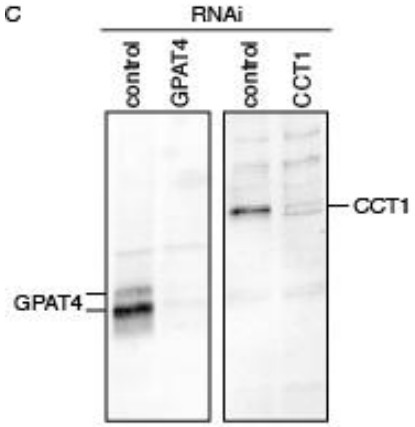

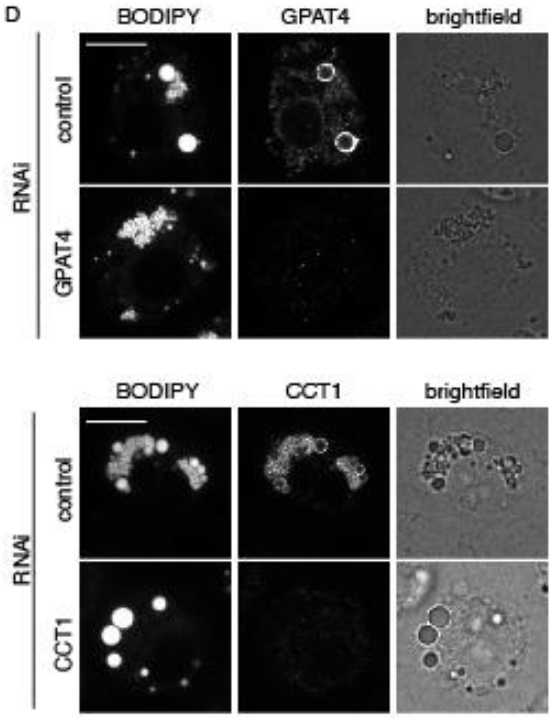

Wilfling et al.
Suppl. Figure 1

A

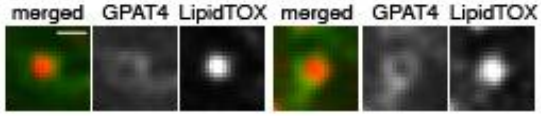

Pearson's correlation coefficient at 30 min		Pearson's correlation coefficient at 3 h	
LD1	0.52	LD6	-0.30
LD2	0.66	LD7	0.17
LD3	0.38	LD8	0.07
LD4	0.55	LD9	0.08
LD5	0.39	LD10	0.20

B

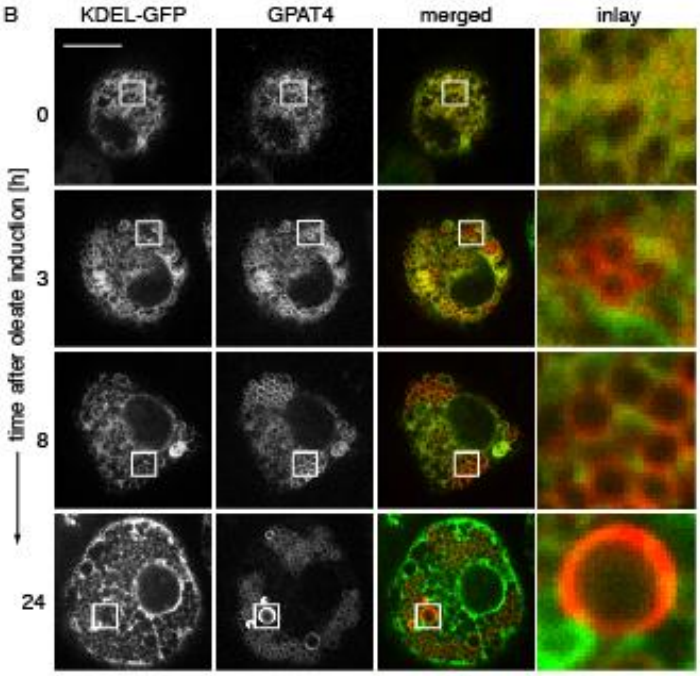

C

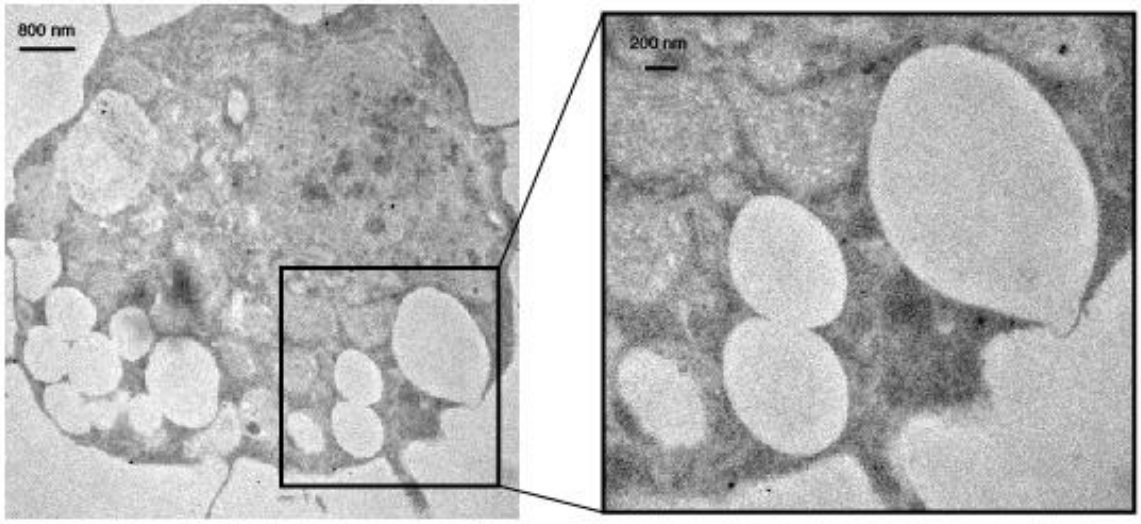

Wilfling et al.
Suppl. Figure 2

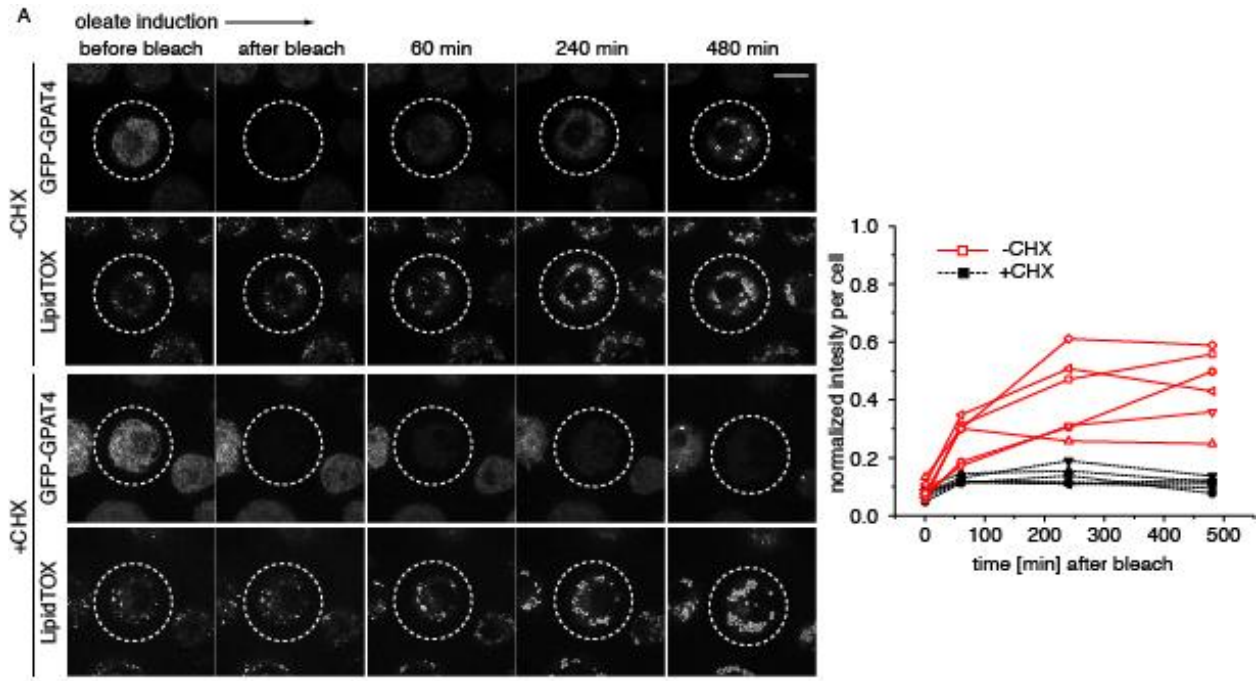

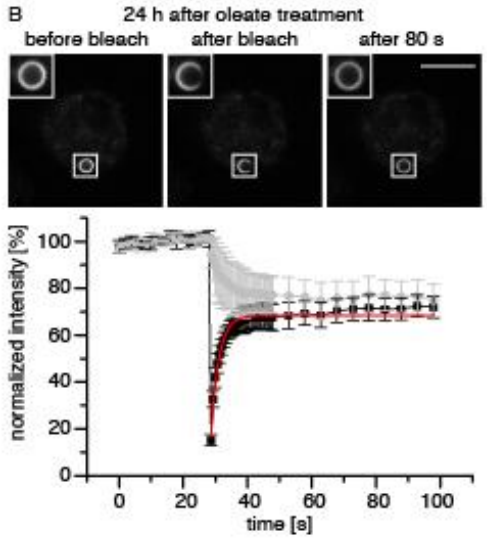

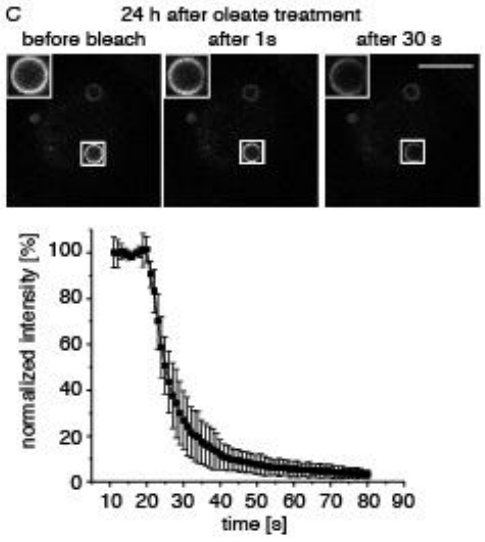

Wilfling et al.
Suppl. Figure 3

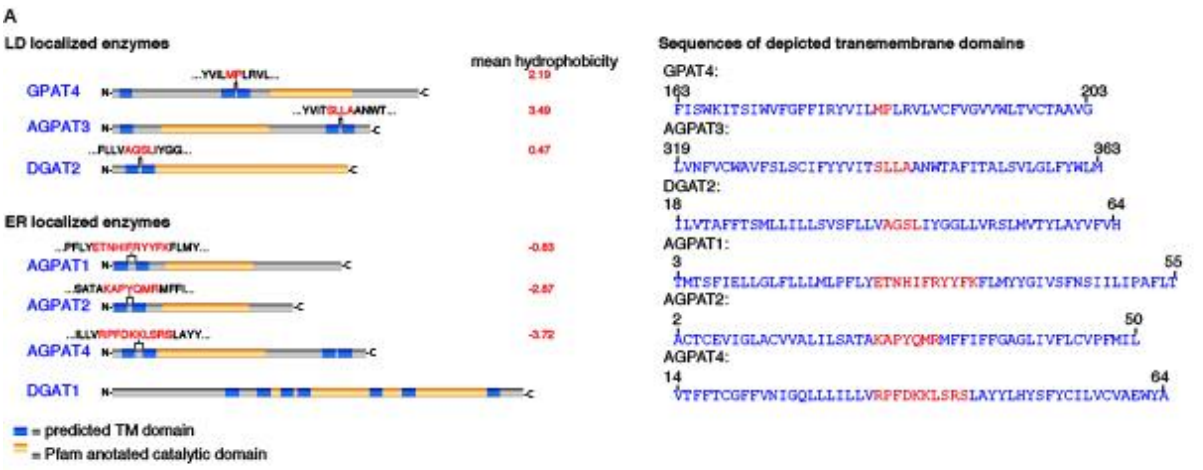

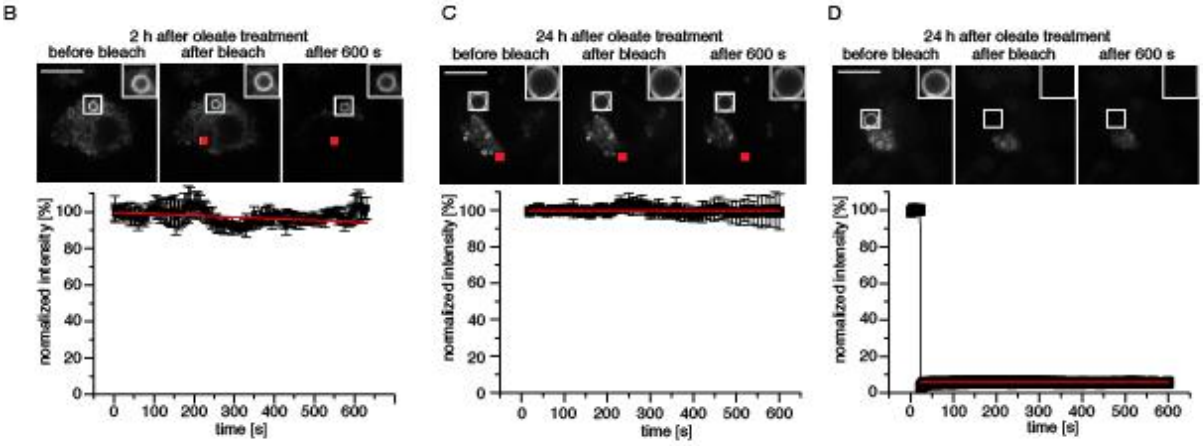

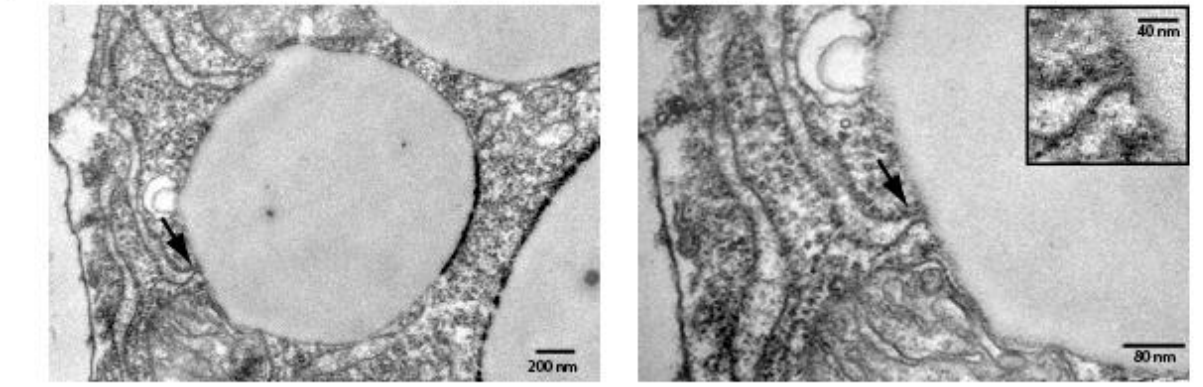

Wilfling et al.
Suppl. Figure 4

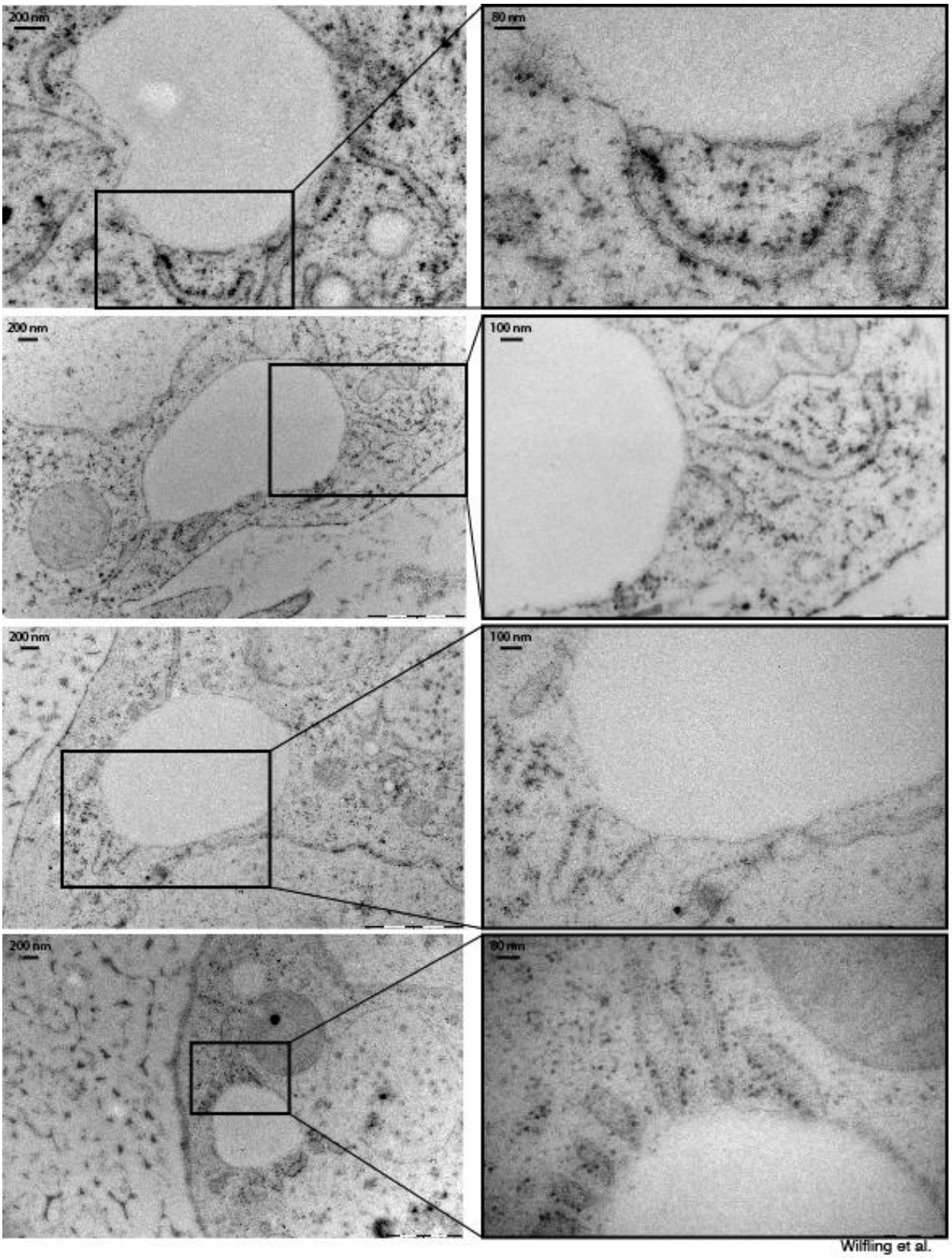

Wilfling et al.
Suppl. Figure 5

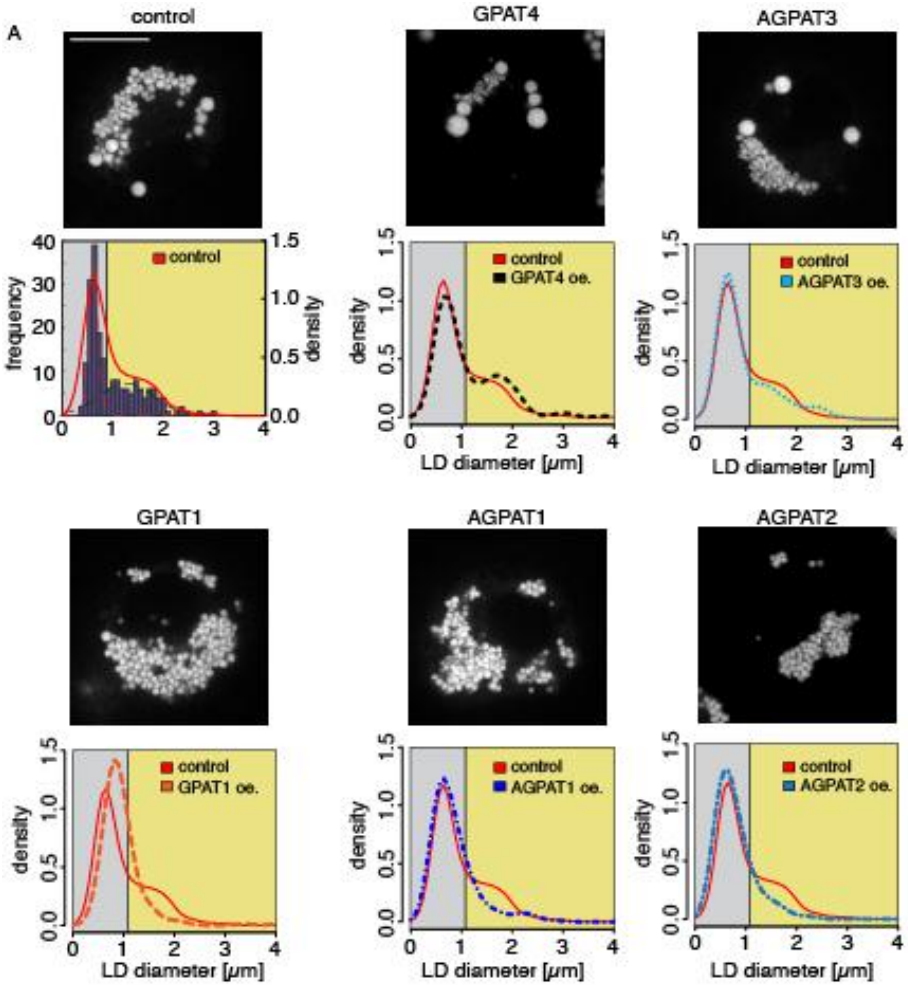

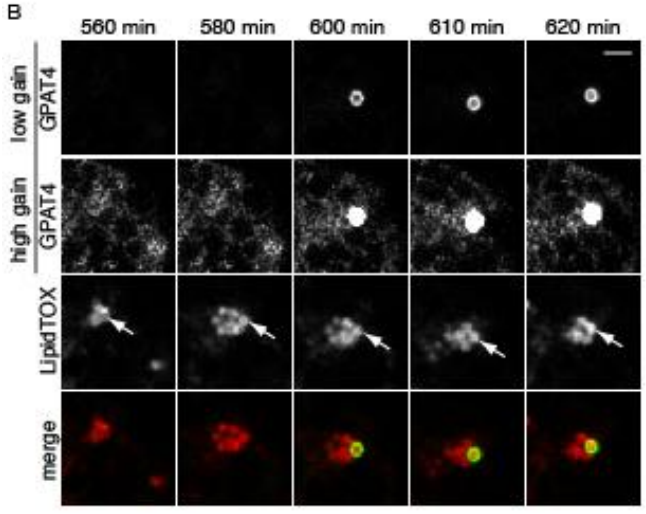

Wilfling et al.
Suppl. Figure 6

Supplemental Figure Legends

Figure S1. A Subset of *de novo* TG Synthesis Enzymes does not Localize to LDs and Specificity of the GPAT4 and CCT1 antibodies, Related to Figure 1

(A) AGPAT1, AGPAT2 or DGAT1 tagged with fluorescent cherry-tag (red) were expressed in *Drosophila* S2 cells grown for 24 h in oleate containing medium, and stained for LDs with BODIPY (green) before imaging. Bar = 10μm (overview) or 1μm (magnification).

(B) AGPAT1/AGPAT2 and DGAT1 are not re-localizing from the ER to LDs. AGPAT1, AGPAT2 or DGAT1 fused to a fluorescent *cherry*-tag (red) were co-expressed with a ER marker (ss-GFP-KDEL; green) in *Drosophila* S2 cells grown for 24h in oleate containing medium and imaged; Bar = 10μm (overview) or 1μm (magnification).

(C and D) Polyclonal antibodies raised in rabbits against GPAT4 and CCT1 specifically recognize their antigen in immunoblots (C) and immunofluorescence (D). Bars = 10μm

Figure S2. GPAT4 Re-localizes from the ER to the LD Surface, Related to Figure 2

(A) GPAT4 accumulates in specialized ER domains at nascent LDs. GPAT4 fused to a fluorescent GFP tag (green) was expressed in *Drosophila* S2 cells grown for 0.5h in oleate containing medium, stained for LDs with LipidTOX (red), and imaged. Bar = 1μm. Pearson correlations coefficients for GFP-Sec61β and CH-GPAT4 signal on LDs at 0.5 or 3h of oleate are shown.

(B) GPAT4 segregates from the ER during LD formation. A time course of LD formation induced by oleate containing medium shows segregation of *cherry*-GPAT4 (red) from the ER marker (ss-GFP-KDEL; green). Bar = 10μm (overview) or 1μm (magnification).

(C) Immunogold labeling on LDs is specific to GPAT4. Thin section electron microscopy samples incubated only with gold –labeled secondary antibodies do not show any signal.

Figure S3. Cycloheximide treatment efficiently blocks GPAT4 synthesis, but not relocalization to LDs and GPAT4 uniformly localizes to LDs, related to Figure 2. .

(A) Cells were either control treated or treated with CHX, and the GPAT4 signal in the indicated circle was bleached at the beginning of the experiment. In the absence of CHX new synthesized GPAT4 is made and relocalizes to LDs, in contrast in the CHX treated cells no new fluorescent GPAT4 is made.

(B) Fluorescence recovery in a bleached region of GFP-GPAT4 signal on mature LDs (after 24 h of incubation with oleate containing medium). Exponentials are shown as curve fits.

Quantitation shows the recovery of GFP-GPAT4 signal from three independent experiments with error bars indicating the standard deviation.

(C) Fluorescence loss in photobleaching (FLIP) of a mature LD after 12 h of incubation with oleate containing medium. The indicated spot (red) is bleached after each image. A linear function (red line) is shown as curve fit. Representative images of one experiment are shown. Bar = 10µm. Quantitation shows the recovery of GFP-GPAT4 signal from three independent experiments with error bars indicating the standard deviation.

Figure S4. Domain Structure of TG Synthesis Enzymes, Related to Figure 3.

(A) Blue bars indicate the position of predicted transmembrane (TM) domains. TOPCONS, SCAMPI, OCTOPUS, and PRO/PRODIV-TMHMM were used for predicting of TMs (http://topcons.cbr.su.se/) in the sequence of the different TG synthesis enzymes. Only TMs predicted by all five programs are displayed. Orange bars indicate the position of the Pfam annotated catalytic domain. Amino acids in the loop region between two predicted transmembrane domains are shown in red and the mean hydrophobicity value for these amino acids was calculated using HydroMCalc (http://www.bbcm.univ.trieste.it/~tossi/HydroCalc/HydroMCalc.html). Lower panel shows the full sequence of the predicted transmembrane domains with the loop region.

(B and C) Fluorescence loss in photobleaching (FLIP) of a mature LD after 2 h (C) and 24 h (D) of incubation with oleate containing medium. The indicated spot (red) is bleached after each image. A linear function (red line) is shown as curve fit. Representative images of one experiment are shown. Quantitation shows the recovery of GFP-GPAT4 signal from three independent experiments with error bars indicating the standard deviation. Bar = 10µm.

(D) GPAT4 is not exchanged between neighboring LDs. Fluorescence recovery of the GFP-GPAT4 signal on a whole, mature LD (after 24 h of incubation with oleate containing medium). Exponentials are shown as curve fits. Quantitation shows the recovery of GPAT4-GFP signal from three independent experiments with error bars indicating the standard deviation. Bar = 10µm

(E) Thin section electron microscopy analysis from chemical fixed samples shows membrane continuity between LDs and the ER.

Figure S5: A Subset of LDs are Connected to the ER, Related to Figure 3.

Thin section electron microscopy analysis from high pressure frozen samples shows membrane continuity between LDs and the ER.

Figure S6: A Subset of LDs are Connected to the ER, Related to Figure 5.

(A) Overexpression of LD-localized TG synthesis enzymes (GPAT4 and AGPAT3) leads to slightly larger LDs, overexpression of mitochondrial- or ER-localized TG synthesis enzymes (GPAT1, AGPAT1 and AGPAT2) leads to small LDs. Representative images and density curves are shown. Bar = 10μm.

(B) LDs can acquire GPAT4 after their initial formation. GFP-GPAT4 was followed by 3D time lapse imaging from 0 to 8h of oleate loading of cells. Bar = 1μm.

Supplemental Tables

Table S1. Proteomic analysis of TG synthesis enzyme targeting to LDs, Related to Figure 1

Protein	Unique Peptides	Ratio H/L S1	Ratio H/L S2	Ratio H/L S3	Ratio H/L S4	Ratio H/L S5	Ratio H/L S6	Ratio H/L S7	Ratio H/L S8	Ratio H/L S9
GRP78	63	2.6149	2.7116	1.1899	0.8548	1.0069	1.5574	1.127	0.6129	2.3185
GAPDH	8	2.2071	0.4240	1.5238	3.2992	4.0112	5.4047	3.7947	3.1275	3.9156
CCT1	26	0.2940	0.0710	0.2037	0.0263	0.0296	0.0810	0.6540	0.4537	1.7191
Acsl1	39	0.7066	0.7605	0.5710	0.0132	0.0140	0.0487	0.4824	0.4494	1.9172
Acsl3	64	0.1132	0.0914	0.0991	0.0082	0.0082	0.0198	0.2512	0.2513	1.1596
GPAT4	20	0.3500	0.3741	0.2931	0.0228	0.0271	0.0618	0.2880	0.4219	2.4509
AGPAT3	21	1.5983	0.2523	0.2173	0.0377	0.0217	0.0314	0.3099	0.3864	0.3633
LIPIN	45	1.6571	0.6723	0.7033	0.1389	0.0644	0.0623	0.3782	0.1511	0.1566

Gene names, the number of unique peptides and the SILAC ratio (indicating purification) are shown (Krahmer et al., 2011).

Table S2. Sequences information of TG synthesis enzymes, Related to Figure 1

CG number	FlyBase ID	human orthologs
CG3961	FBgn0036821	ACSL1
CG8732	FBgn0263120	ACSL3
CG5508	FBgn0027579	GPAT1
CG3209	FBgn0034971	GPAT4
CG3812	FBgn0030421	AGPAT1
CG17608	FBgn0026718	AGPAT2
CG4729	FBgn0036623	AGPAT3
CG4753	FBgn0036622	AGPAT4

CG8709	FBgn0263593	LIPIN
CG31991	FBgn0004797	DGAT1
CG1942	FBgn0033215	DGAT2

Table S3. Mass spectrometry data for GPAT4 Pull-down, related to Figure 6. Averaged peptide Intensities (LFQ) for each protein (ProteinIDs and Gene Name) detected in the different replicates +/- oleate (+/- OA) are shown derived as described in (Hubner et al., 2010). In addition, the number of total peptides, unique peptides, the p-value for the test of significance between conditions, as well as the log2 of the abundance ration between oleate and non oleate treated conditions are shown. Available separately online.

Supplemental Experimental Procedures

Plasmid DNA Construction

Full-length cDNA encoding CG3209 (GPAT4), CG3812 (AGPAT1), CG17608 (AGPAT2), CG31991 (DGAT1), CG1942 (DGAT2), or CG10130 (SEC61β) was cloned from cDNA clones obtained from the DGRC (https://dgrc.cgb.indiana.edu/) and subcloned into the pENTR™/SD/D-TOPO vector (Invitrogen). The hairpin constructs CG3209 160-216 and CG3209 160-216 w loop of AGPAT1 (CG3812) were obtained by gene-synthesis from Invitrogen and subcloned into the pENTR™/SD/D-TOPO vector (Invitrogen). CG3209 with the replaced hairpin by a flexible linker was obtained by fusion PCR. The entry clone was further subcloned into the different destination expression vectors (actin promoter). The destination vectors used in this study are part of the Drosophila Gateway™ Vector Collection and are available from the DGRC (https://dgrc.cgb.indiana.edu/).

Sequences of primers used for RNAi experiments

Gene	Gene ID	Forward	Reverse
GPAT1	CG5508	AACCT1GCAAATTCCGGTCT	CAGATGGCTTGTAGACCT1TG
GPAT4	CG3209	CGGCGACGCCTTCTG	CAGCCGATTGGCAAACTC
AGPAT1	CG3812	TTATCGAACTGCTGGGACT	GCGGACATCGCATGGTC
AGPAT2	CG17608	GCTCCCAAAAATGGCTTGTA	GAACGCAAAGATCAACAGCA
AGPAT3	CG4729	GAGTTTGCTGCATGGAAAG	AGTCCCAGGACGGAAAGT
AGPAT4	CG4753	TTTGCGGAAAAGGACAAGAT	ACAGCGTATTCCATGAGGCT
LIPIN	CG8709	GTGGTGCTGGGTCAGGTC	TCCCT1CTGCTGCTTGGT
DGAT1	CG31991	AACCGCAAGTCAACACAAAA	AAGCCCAAACGCAGACC
DGAT2	CG1942	CAAGTGGCTGGAGCTATTC	GGATCAGCGCCT1CTTTG
CCT1	CG1049	ACATCTATGCTCCT1CTCAAGGC	CTCTGCAGACTCTGGTAACTGC
pBluescript		AATTCGATATCAAGCTTATCGAT	TAAATTGTAAGCGTTAATATTTTG

Cell Culture and Transfection

WT *Drosophila* S2 or stably pAGW-GPAT4 transfected cells were cultured, treated with oleate, transfected and depleted by RNAi as described (Krahmer et al., 2011). Cells were analyzed after 5–8 days of RNAi treatment. Table S2 contains a list of primers to generate dsRNAs for RNAi. A segment of pBluescript backbone was used as the template for control RNAi. Bone marrow-derived macrophages from wt and *Gpat4*-/- mice were isolated and cultured as

described in (Weischenfeldt and Porse, 2008). Mouse embryonic fibroblasts (MEFs) were derived from E14 embryos of wt, *Dgat1-/-* or *Dgat2-/-* mice as described previously (Zhang et al., 2004). MEFs and McArdle RH7777 cells were cultured in DMEM with 10% FBS and 10% horse serum. Before imaging, cells were split onto glass bottom plates and incubated in the culture media supplemented with 500µM oleate overnight.

Antibodies

dGPAT4 (CG3209) was detected with a rabbit polyclonal antibody raised against the peptide CWDGQLKRMKPKKEWREIQQ (aa 428–446). CCT1 (CG1049) was detected with a rabbit polyclonal antibody raised against the peptide CSGSLNGKQRPKQKRSSLAR (aa 471–494). Both antibodies were affinity purified using the corresponding peptide coupled to SulfoLink coupling resin (Thermo Scientific). dGRP78 was detected using a commercial antibody against GRP78/BiP (ET-21) (Sigma-Aldrich). dTubulin was detected using a commercial mouse monoclonal antibody raised against tubulin (Sigma-Aldrich). For co-staining of dGPAT4 and dCCT1, both antibodies were biotinylated using the EZ-Link NHS-PEG4 biotinylation kit (Thermo Scientific).

Supplemental References

Hubner, N.C., Bird, A.W., Cox, J., Splettstoesser, B., Bandilla, P., Poser, I., Hyman, A., and Mann, M. (2010). Quantitative proteomics combined with BAC TransgeneOmics reveals in vivo protein interactions. J Cell Biol *189*, 739-754.

Krahmer, N., Guo, Y., Wilfling, F., Hilger, M., Lingrell, S., Heger, K., Newman, H.W., Schmidt-Supprian, M., Vance, D.E., Mann, M.*, et al.* (2011). Phosphatidylcholine synthesis for lipid droplet expansion is mediated by localized activation of CTP:phosphocholine cytidylyltransferase. Cell Metab *14*, 504-515.

Weischenfeldt, J., and Porse, B. (2008). Bone Marrow-Derived Macrophages (BMM): Isolation and Applications. CSH protocols *2008*, pdb prot5080.

Zhang, J., Fu, M., Cui, T., Xiong, C., Xu, K., Zhong, W., Xiao, Y., Floyd, D., Liang, J., Li, E.*, et al.* (2004). Selective disruption of PPARgamma 2 impairs the development of adipose tissue and insulin sensitivity. Proceedings of the National Academy of Sciences of the United States of America *101*, 10703-10708.